

Prediction of site-specific amino acid distributions and limits of divergent evolutionary changes in protein sequences

Markus Porto,¹ H. Eduardo Roman,² Michele Vendruscolo,³ and Ugo Bastolla⁴

¹*Institut für Festkörperphysik, Technische Universität Darmstadt, Hochschulstr. 8, 64289 Darmstadt, Germany*

²*Dipartimento di Fisica and INFN, Università di Milano, Via Celoria 16, 20133 Milano, Italy*

³*Department of Chemistry, University of Cambridge, Lensfield Road, Cambridge CB2 1EW, UK*

⁴*Centro de Astrobiología (INTA-CSIC), 28850 Torrejón de Ardoz, Spain*

(Dated: March 26, 2004, revised October 15, 2004)

We derive an analytic expression for site-specific stationary distributions of amino acids from the Structurally Constrained Neutral (SCN) model of protein evolution with conservation of folding stability. The stationary distributions that we obtain have a Boltzmann-like shape, and their effective temperature parameter, measuring the limit of divergent evolutionary changes at a given site, can be predicted from a site-specific topological property, the principal eigenvector of the contact matrix of the native conformation of the protein. These analytic results, obtained without free parameters, are compared with simulations of the SCN model and with the site-specific amino acid distributions obtained from the Protein Data Bank. These results also provide new insights into how the topology of a protein fold influences its designability, i.e. the number of sequences compatible with that fold. The dependence of the effective temperature on the principal eigenvector decreases for longer proteins, a possible consequence of the fact that selection for thermodynamic stability becomes weaker in this case.

I. INTRODUCTION

The reconstruction of phylogenetic distances from sequence alignments requires the use of a model of protein evolution. Evolutionary models are also needed for reconstructing phylogenetic trees in the framework of maximum likelihood methods (Felsenstein, 1981). In this context, both the mutational process and the selection on protein folding and function must be taken into account. It is well known that the local environment of a protein site within the native structure influences the probability of acceptance of a mutation at that site (Overington et al., 1990). Nevertheless, structural biology still has a very limited impact in studies of phylogenetic reconstruction, and the models commonly used in these studies rely on substitution matrices that do not consider the structural specificity of different sites. The most used substitution matrices, such as JTT (Jones et al., 1992), are obtained extrapolating substitution patterns observed for closely related sequences, and they have low performances when distant homologs are concerned (Henikoff and Henikoff, 1993).

To take into account the protein-level selection, it is necessary to consider site-specific amino acid distributions within a protein family (Halpern and Bruno, 1998). Similarly, the use of site-specific substitution matrices improves substantially maximum likelihood methods for reconstructing phylogenetic trees (Liò and Goldman, 1998; Thorne, 2000; Fornasari et al., 2002).

In the studies mentioned above, site-specific constraints are obtained through simulations of a model of protein evolution. In this work we derive an analytic expression, without adjustable parameters, for site-specific amino acid distributions and show that they are in very good agreement with simulations of a model of protein evolution and with site-specific amino acid distributions obtained from the Protein Data Bank.

The site-specific conservation patterns that we predict are associated with a key topological indicator of native state topology, namely the principal eigenvector of the contact matrix (Bastolla et al., 2004; Porto et al., 2004). Our approach is based on the Structurally Constrained Neutral model (SCN model; Bastolla et al., 1999, 2000a, 2002, 2003a, 2003b),

where possible mutations are tested for conservation of structural stability using a computational model of protein folding (Bastolla et al., 1998, 2000b, 2001). This approach is similar in spirit to the Structurally Constrained Protein Evolution model (SCPE; Parisi and Echave, 2001), that uses a different criterion to assess the thermodynamic stability. Notice that the SCN model does not assume independence at different sites, and in fact we have recently shown that site-dependence is linked to a rather debated feature of neutral evolution, the overdispersion of neutral substitutions (Bastolla et al., 2003b).

The analytical prediction that we derive in this paper also allows site-specific conservation across protein families to be calculated. As we have previously shown (Bastolla et al., 2003a), the site-specific conservation patterns provided by the SCN model match qualitatively structural conservation patterns found in bioinformatics studies (Ptitsyn, 1998; Ptitsyn and Ting, 1999).

Further, the site-specific amino acid distribution that we present here also enables us to derive an estimate of the sequence entropy compatible with a given fold, which is termed the ‘designability’ of the fold (Li et al., 1998; Helling et al., 2001). These results are in agreement with recent studies suggesting that the designability can be inferred from the protein topology alone (Koehl and Levitt, 2002; England and Shakhnovich, 2003).

II. BACKGROUND

In the SCN model (Bastolla et al., 2002, 2003a), starting from the protein sequence in the Protein Data Bank (PDB), amino acid mutations are randomly performed and accepted according to a stability criterion based on an effective model of protein folding (Bastolla et al., 2000b, 2001). We use a coarse-grained representation of protein structures as a binary contact matrix C_{ij} with elements equal to one if i and j are in contact (at least one pair of heavy atoms, one belonging to each amino acid, are less than 4.5 Å apart), and zero otherwise. The effective free energy for a sequence \mathbf{A} in configuration \mathbf{C} is approximated by an effective contact free energy

function $E(\mathbf{A}; \mathbf{C})$,

$$\frac{E(\mathbf{A}; \mathbf{C})}{k_B T} = \sum_{i < j} C_{ij} U(a_i; a_j); \quad (1)$$

where \mathbf{U} is a 20×20 symmetric matrix with $U(a; b)$ representing the effective interaction, in units of $k_B T$, of amino acids a and b when they are in contact; we use the interaction matrix derived by Bastolla et al. (2001). The free energy function, Eq. (1), assigns lowest free energy to the experimentally known native structure against decoys generated by threading the sequence over protein-like structures derived from the PDB. If gaps in the sequence-structure alignment are allowed, one has to use a suitable gap penalty term.

For testing the stability of a protein conformation, we use two computational parameters: (i) The effective energy per residue, $E(\mathbf{A}; \mathbf{C}) = N$, where N is the protein length, which correlates strongly with the folding free energy per residue for a set of 18 small proteins that are folding with two-states thermodynamics (correlation coefficient 0.91; U. Bastolla, unpublished result); (ii) The normalized energy gap α , which characterizes fast folding model sequences (Bastolla et al., 1998) with well correlated energy landscapes (Bringelson and Wolynes, 1987; Goldstein et al., 1992; Abkevich et al., 1994; Gutin et al., 1995; Klimov and Thirumalai, 1996). A mutated sequence is considered thermodynamically stable if both computational parameters are above predetermined thresholds (Bastolla et al., 2003a).

The interaction matrix \mathbf{U} can be written in spectral form as $U(a; b) = \sum_{\alpha=1}^{20} \varepsilon_{\alpha} u^{(\alpha)}(a) u^{(\alpha)}(b)$, where ε_{α} are the eigenvalues, ranked by their absolute value, and $\mathbf{u}^{(\alpha)}$ are the corresponding eigenvectors. The main contribution to the interaction energy comes from the principal eigenvector $\mathbf{u}^{(1)}$, which has a negative eigenvalue $\varepsilon_1 < 0$, as $\varepsilon_1 u^{(1)}(a) u^{(1)}(b)$ has correlation coefficient 0.81 with the elements $U(a; b)$ of the full matrix. It is well known that hydrophobic interactions determine the most significant contribution to pairwise interactions in proteins, so that the components of the main eigenvector are strongly correlated with experimental hydrophobicity scales (Casari et al., 1992; Li et al., 1997). Considering only this main component, we define an approximate effective energy function $H(\mathbf{A}; \mathbf{C})$, yielding a good approximation to the full contact energy, Eq. (1),

$$\frac{H(\mathbf{A}; \mathbf{C})}{k_B T} = \alpha \sum_{i < j} C_{ij} h(A_i) h(A_j); \quad (2)$$

We call $\mathbf{h}(\mathbf{A}) = \mathbf{u}^{(1)}(\mathbf{A})$ the Hydrophobicity Profile (HP) of sequence \mathbf{A} (Bastolla et al., 2004). This is an N -dimensional vector whose i -th component is given by $h(A_i) = u^{(1)}(A_i)$. The 20 parameters $h(a) = u^{(1)}(a)$ are obtained from the principal eigenvector of the interaction matrix, and we call them *interactivity parameters*.

The HP provides a vectorial representation of protein sequences. In turn, a convenient vectorial representation of protein structures may be obtained by the principal eigenvector of the contact matrix \mathbf{C} , which we denote by PE and we indicate by \mathbf{c} . This vector maximizes the quadratic form $\sum_{i,j} C_{ij} c_i c_j$ with the constraint $\sum_i c_i^2 = 1$. In this sense, c_i can be interpreted as the effective connectivity of position i , since positions with large c_i are in contact with as many as possible

positions j with large c_j . All its components have the same sign, which we choose by convention to be positive. Moreover, if the contact matrix represents a single connected graph (as it does for single-domain globular proteins), the information contained in the principal eigenvector is sufficient to reconstruct the whole contact matrix (Porto et al., 2004).

For any given protein fold, identified through its PE, we can define the optimal HP, \mathbf{h}_{opt} , as the HP that minimizes the approximate effective free energy, Eq. (2), for fixed mean and squared mean of the hydrophobicity vector, $h = N^{-1} \sum_i h(A_i)$ and $h^2 = N^{-1} \sum_i h(A_i)^2$. We impose a condition on the mean hydrophobicity, h , because, if a sequence is highly hydrophobic, not only the native structure but also alternative compact structures will have favorable hydrophobic energy. Selection to maintain a large normalized energy gap is therefore expected to place constraints on the value of h .

From the above property of the PE, \mathbf{c} , it is clear that the optimal HP, \mathbf{h}_{opt} , is strongly correlated with the PE (Bastolla et al., 2004). In this formulation, h and h^2 are not determined by the native structure but depend on the mutation and selection process (see below).

The optimal HP constitutes an analytic solution to the sequence design problem with energy function given by Eq. (2), and an approximate solution to sequence design with the full contact energy function, Eq. (1). In the SCN evolutionary model, attempted mutations are accepted whenever the effective free energy and the normalized energy gap overcome pre-defined thresholds. Therefore, we do not expect that the optimal HP is ever observed during evolution, but we do expect thermodynamically stable sequences compatible with a given fold to have HPs distributed around the optimal one. We have verified this prediction, finding that the HPs of individual selected sequences are correlated with the principal eigenvector of the protein fold with correlation coefficient of 0.45 (averaged over seven protein folds and over hundred thousands of simulated sequences per fold), whereas the HP averaged over all sequences compatible with a given fold, \mathbf{h}_{evol} , correlates much more strongly with the principal eigenvector of that fold, with mean correlation coefficient 0.96 averaged over the same seven folds (Bastolla et al., 2004). These results show that one can recover the optimal HP through an evolutionary average of the HPs compatible with the protein fold.

We found a similar result for the protein families represented in the PFAM (Bateman et al., 2000) and in the FSSP (Holm and Sander, 1996) databases. In this case, however, the correlation between the principal eigenvector and the evolutionary average of the HP is weaker: The average correlation coefficient is 0.57 for PFAM families and 0.58 for FSSP families (Bastolla et al., 2004). This weaker correlation is not unexpected, since functional conservation, which is not accounted for in the SCN model, plays an important role in protein evolution, and the effective energy function that we use to test thermodynamic stability is only an approximation. In addition, the number of sequences used to calculate the average HP in the PFAM and FSSP databases is much smaller than the number of sequences obtained by the SCN model. When the average HP is computed using only some hundreds of SCN sequences, the same order of magnitude as in PFAM or FSSP families, the correlation with the principal eigenvector also drops to values comparable to those observed for the

PFAM and the FSSP sequence databases.

III. RESULTS

A. Derivation of $\pi_i(a)$

The results presented above suggest that the SCN model of protein evolution can be represented as a trajectory in sequence space where the HP moves around the optimal HP, which is strongly correlated with the principal eigenvector of the protein fold's contact matrix (Bastolla et al., 2004). In this work, we use this analogy to compute analytically the site-specific distribution of amino acid occurrences $\pi_i(a)$, where i indicates a protein position and a indicates one of the 20 amino acid types.

Our previous results indicate that the evolutionary average of the hydrophobicity vector, \mathbf{h}_{evol} , is correlated with the principal eigenvector \mathbf{c} of the native contact matrix. In order to derive an analytical expression for $\pi_i(a)$, we now assume that the correlation coefficient between the principal eigenvector and the average HP is 1, i.e. $r(\mathbf{h}_{\text{evol}}; \mathbf{c}) = \mathbf{h}_{\text{evol}} \cdot \mathbf{c}$

$h_{\text{evol}} \cdot c = \sigma_c \sigma_{h_{\text{evol}}} = 1$, and we obtain

$$h_i_{\text{evol}} \sum_{\text{fag}} \pi_i(a) h(a) = A c_i = c - 1 + B; \quad (3)$$

where the sum over fag is over all amino acids, and

$$A = \frac{1}{\tau} \frac{\sum_{\text{fag}} h_{\text{evol}}^2}{c^2} \quad \text{and} \quad B = h_{\text{evol}} : \quad (4)$$

We are representing here two kinds of average: The angular brackets denote the average over the N positions of the protein, $f = N^{-1} \sum_i f_i$, and the corresponding standard deviation is denoted by $\sigma_f^2 = f^2 - f^2$, whereas square brackets denote position-specific evolutionary averages, $f_{\text{evol}} = \sum_{\text{fag}} \pi_i(a) f(a)$.

Eqs. (3,4) are the conditions that the stationary distributions $\pi_i(a)$ have to fulfill in order to guarantee a perfect correlation between principal eigenvector and the average HP. We assume that these conditions are the only requirement that the $\pi_i(a)$ have to meet, so that at stationarity the $\pi_i(a)$ are the distributions of maximal entropy compatible with the above conditions. It is well known that the solution of this optimization problem are Boltzmann-like (exponential) distributions, characterized by an effective ‘temperature’ β_i that, in this context, varies from site to site and measures the tolerance of site i to accept mutations over very long evolutionary times,

$$\pi_i(a) = \frac{\exp[-\beta_i h(a)]}{\sum_{\text{fag}} \exp[-\beta_i h(a)]}; \quad (5)$$

with the constraint, Eq. (3),

$$\sum_{\text{fag}} \exp[-\beta_i h(a)] h(a) = A c_i = c - 1 + B = 0; \quad (6)$$

Eq. (6) states an analytical relation between the ‘Boltzmann parameter’ β_i and the principal eigenvector component c_i , given the two evolutionary parameters A and B . One

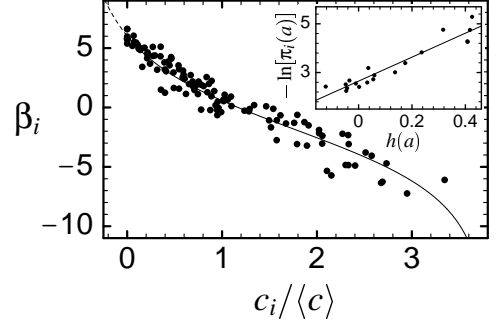


FIG. 1: ‘Boltzmann parameter’ β_i as a function of the scaled principal eigenvector component $c_i = c$ as obtained by the SCN model for ribonuclease (PDB id. 7rsa). The line shows the analytical prediction, Eq. (7), obtained using the mean hydrophobicity $h_{\text{evol}} = 0.108$ and the variance $h_{\text{evol}}^2 = 0.0077$ as observed in the simulations of the SCN model. The dashed part of the curve indicates the forbidden area $c_i < 0$. The inset exemplifies the numerical obtained $\ln \pi_i(a)$ vs hydrophobicity $h(a)$ of amino acid a , as obtained for ribonuclease at protein position $i = 50$ (with $c_{50} = c = 0.124$), yielding $\beta_{50} = 4.92$.

sees from this equation that β_i equals zero if $c_i = c = 1 + A^{-1} \sum_{\text{fag}} h(a) = 20 h_{\text{evol}}$, and β_i becomes negative for larger c_i and positive for smaller c_i . We expect that the relationship between β_i and c_i is almost linear in the range $c_i = c - 1 \dots 1$, whereas β_i tends to minus infinity when the average hydrophobicity at site i , h_i_{evol} , tends to the maximally allowed value, and to plus infinity when the average hydrophobicity at site i tends to the minimum allowed value.

Eq. (6) can be interpreted as follows: (i) Positions with large eigenvector component c_i are buried in the core of the protein and are therefore with high probability occupied by hydrophobic amino-acids (positive $h(a)$) and have large and negative β_i , (ii) surface positions with small c_i are more likely occupied by polar amino acids (negative $h(a)$) and have large and positive β_i , and (iii) intermediate positions are the most tolerant having a small negative or small positive β_i .

B. Validation: SCN model

We first verified these predictions using the simulated trajectories obtained through the SCN model. We found that the site-specific stationary distributions of amino acids, $\pi_i(a)$, are well fitted by an exponential function of hydrophobicity, $\pi_i(a) \propto \exp[-\beta_i h(a)]$, where we use the interactivity scale given by the main eigenvector of our interaction matrix.

Analytically, the expected site-dependent Boltzmann parameter β_i can be calculated in an implicit form by rewriting Eq. (6) as

$$c_i = c = 1 + A^{-1} \frac{\sum_{\text{fag}} h(a) \exp[-\beta_i h(a)]}{\sum_{\text{fag}} \exp[-\beta_i h(a)]} \quad ; \quad (7)$$

giving c_i as a function of β_i . To obtain β_i as a function of c_i , Eq. (7) has to be inverted numerically, and the parameters A and B are obtained from the simulation data by Eq. (4).

The predictions derived in this way, for the ribonuclease

Protein	PDB id.	N	β	R	r
rubredoxin (mesophilic)	1iro	53	0.98	0.96	0.96
rubredoxin (thermophilic)	1brf_A	53	0.98	0.96	0.97
SH3 domain	1aey	58	0.93	0.97	0.95
cytochrome c	451c	82	0.94	0.84	0.84
ribonuclease	7rsa	124	0.94	0.83	0.89
lysozyme	3lzt	129	0.93	0.73	0.82
myoglobin	1a6g	151	0.95	0.94	0.88
ubiquitin conjugating enzyme	1u9a_A	160	0.90	0.88	0.79
TIM barrel	7tim_A	247	0.94	0.88	0.84
kinesin	1bg2	323	0.87	0.79	0.73

TABLE I: Correlation coefficients between site-specific quantities predicted using the equations derived in this work and observed in SCN simulations. Fourth column: ‘Boltzmann parameters’ β . Fifth column: Rigidities R . Sixth column: Substitution rates r . Note that sites containing cysteine residues are not included in the calculation of the correlation coefficients, as cysteine residues form pairwise disulphide bridges (which are very poorly represented through hydrophobicity) and are strictly conserved in our evolutionary model.

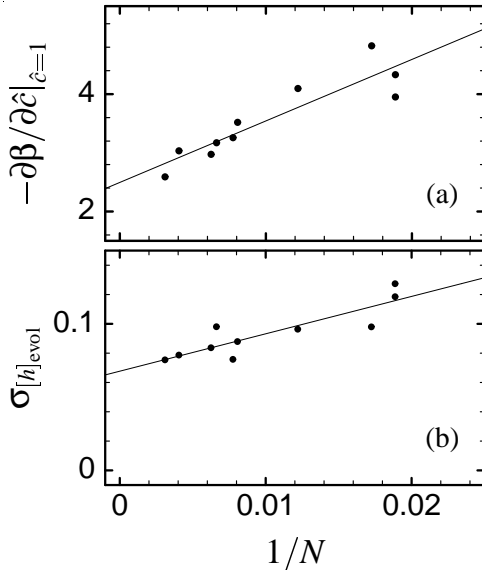


FIG. 2: (a) Plot of slope $-\partial\beta/\partial\hat{c}$, with $\hat{c} = c$ obtained at $\hat{c} = 1$, vs inverse chain length $1/N$. The line shows a fit of the form $A_0 + A_1 = N$. (b) Plot of the standard deviation of the hydrophobicity, $\sigma[h]_{\text{evol}}$, vs inverse chain length $1/N$ as obtained by the SCN model. The line shows a fit of the form $B_0 + B_1 = N$.

fold (PDB id. 7rsa), are compared in Fig. 1 to the β_i obtained by fitting the distributions π_i (a) simulated through the SCN model. The prediction does not involve any adjustable parameter, since A and B are calculated from h_{evol} and h_{evol}^2 as determined by the results of the SCN model. The latter values do not depend on the native structure, but they depend generally on the mutation and selection process, and specifically on its realization as simulated through the SCN model. The other proteins studied show a similar behavior, and the mean correlation coefficient between predicted and observed β_i is 0.935 (cf. Table I).

One notices from Fig. 1 that β_i depends almost linearly

on the scaled principal eigenvector component $c_i = c$ over a wide range of values. The slope of this linear part, the derivative $\partial\beta/\partial\hat{c}$ taken at $\hat{c} = c = 1$, scales with length N , and it can be well fitted by the expression $A_0 + A_1 = N$ with $A_0 = 2.50 \pm 0.21$ and $A_1 = 104.8 \pm 9.2$ for the proteins listed in Table I, see Fig. 2(a). One sees from this expression that, as the protein length increases, the Boltzmann parameter β_i becomes less dependent on $c_i = c$ and therefore more homogeneous. This result, at first sight unexpected, can be better understood considering Eq. (7), which implies that the derivative of β_i with respect to $\hat{c} = c$ is proportional to the standard deviation of the hydrophobicity,

$$\frac{\partial\beta}{\partial\hat{c}}|_{\hat{c}=0} \propto \frac{1}{\sqrt{c^2 - c^2}} \frac{\sigma[h]_{\text{evol}}^2}{h_{\text{evol}}^2} : \quad (8)$$

The standard deviation of the hydrophobicity, measured from simulations of the SCN model, decreases as a function of chain length as $B_0 + B_1 = N$ with $B_0 = 0.068 \pm 0.016$ and $B_1 = 2.55 \pm 0.17$, see Fig. 2(b). Thus, site-specificity decreases for longer proteins because the evolutionary average of the HP becomes more homogeneous across different positions. This result can be explained by noticing that not only the standard deviation, but also the mean hydrophobicity, h_{evol} , decreases as a function of chain length (notice again the two kinds of average). So, the result that site-dependent Boltzmann parameters become more homogeneous for longer proteins ultimately depends on the fact that longer proteins tend to be less hydrophobic.

C. Validation: PDB structures

We compared our predictions to site-specific distributions obtained from a representative subset of the Protein Data Bank (PDB). We considered a non-redundant subset of single-domain globular proteins in the PDB, with a sequence identity below 25% (Hobohm and Sanders, 1994). Globularity was verified by imposing that the fraction of contacts per residue was larger than a length dependent threshold, $N_c = N > 3.5 + 7.8N^{-1/3}$. This functional form represents the scaling of the number of contacts in globular proteins as a function of chain length (the factor $N^{-1/3}$ comes from the surface to volume ratio), and the two parameters were chosen so as to eliminate outliers with respect to the general trend, which are mainly non-globular structures. The condition of being single-domain was verified by imposing that the normalized variance of the PE components was smaller than a threshold,

$1 - N c^2 = N c^2 < 1.5$. Multi-domain proteins have PE components which are large inside their main domains and small outside them. The PE components would be exactly zero outside the main domains if the domains do not share contacts. Therefore, multi-domain proteins are characterized by a larger normalized variance of PE components with respect to single-domain ones. We have verified that the threshold of 1.5 is able to eliminate most of the known multi-domain proteins and very few of the known single-domain proteins (data not shown).

We thus selected 774 sequences of various lengths, 404 of which were shorter than 200 amino acids. We first considered

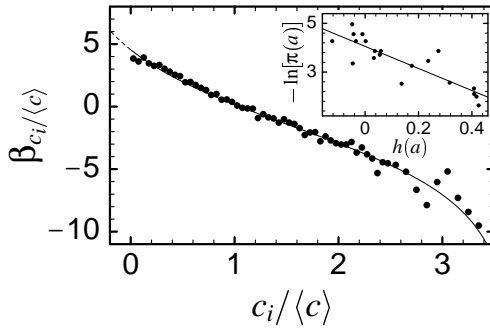


FIG. 3: ‘Boltzmann parameter’ $\beta_{c_i=hc_i}$ as a function of the scaled principal eigenvector component $c_i = c$ as obtained by analyzing a subset of 404 non-redundant single-domain globular structures of the PDB. The line shows the analytical prediction, Eq. (9), obtained using the mean hydrophobicity $h_{\text{PDB}} = 0.128$ and the variance $h_{\text{PDB}}^2 - h_{\text{PDB}}^2 = 0.009$ as obtained from this set. The dashed part of the curve indicates the forbidden area $c_i < 0$. The inset exemplifies the numerically obtained $\ln[\pi(a)]$ vs hydrophobicity $h(a)$ of amino acid a , as obtained for $c_i = c$ [245, 251] yielding $\beta = -4.53$.

only this subset of short proteins, and then the whole data set, divided in bins of similar lengths. We counted the number of each of the 20 amino acids as a function of $c_i = c$, where c denotes the average over a single structure. We used a bin-size of 0.05 for $c_i = c$ [25] and a bin-size of 0.1 for $c_i = c$ > 2.5. Then, for each bin of $c_i = c$, we fitted the observed distributions $\pi_{c_i=hc_i}(a)$ with an exponential function of the hydrophobicity parameters, $\pi_{c_i=hc_i}(a) \propto \exp[-\beta_{c_i=hc_i} h(a)]$. As in the case of the SCN simulations, we used the interactivity scale derived from our effective free energy function. The exponential fit was sufficiently good, and yielded the observed Boltzmann parameters as a function of the normalized PE components.

Next we calculated the predicted Boltzmann parameters through the equation:

$$c_i = c = 1 + \tilde{A}^{-1} \frac{\sum_{\text{fag}} h(a) \exp[-\beta_{c_i=hc_i} h(a)]}{\sum_{\text{fag}} \exp[-\beta_{c_i=hc_i} h(a)]} \quad ; \quad (9)$$

with the parameters \tilde{A} and \tilde{B} now given by

$$\tilde{A} = \frac{V}{\tau} \frac{h_{\text{PDB}}^2 c_i=hc_i}{c^2} \quad \text{and} \quad \tilde{B} = h_{\text{PDB}} c_i=hc_i; \quad (10)$$

where the square brackets h_{PDB} now denote, instead of the evolutionary average over a protein family, the average over all positions with fixed $c_i = c$, even belonging to different structures, whereas angular brackets, $h_{\text{PDB}} c_i=hc_i$, denote the average over all values of $c_i = c$. The denominator $c^2 = c_{\text{PDB}}^2$ indicates the quantity $c^2 = c_{\text{PDB}}^2$, obtained individually for each structure, averaged over the whole set of structures.

The observed Boltzmann parameters are compared in Fig. 3 to the predictions of Eq. (9). Notice that the agreement is

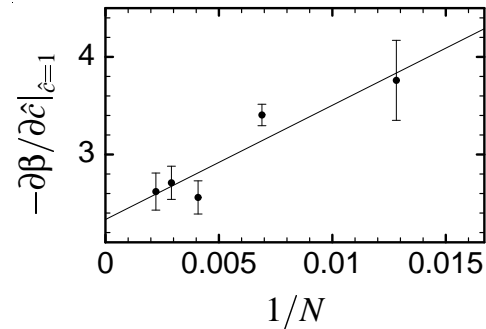


FIG. 4: Plot of slope $-\partial\beta/\partial\hat{c}$, with $\hat{c} = c$ obtained at $\hat{c} = 1$, vs inverse chain length $1/N$, obtained for structures of different length in the PDB.

indeed remarkable, as the predictions do not involve any adjustable parameter, since \tilde{A} and \tilde{B} are calculated from the PDB data.

We stated in the previous section that, with SCN data, the dependence of the Boltzmann parameters on the PE components becomes weaker, and the amino acid distributions become more homogeneous, for longer chains. We tested whether this interesting observation also holds for site-specific distributions obtained from the PDB. To this end, we divided our set of proteins in five bins of proteins with less than 100, 200, 300, 400, and 500 amino acids, respectively, and we measured the dependence of the Boltzmann parameters on the PE component for each bin. From these data, we obtained the derivative of the Boltzmann parameters at $\hat{c} = c = 1$ simply by fitting a straight line to $\beta(\hat{c})$ for \hat{c} in the range between 0.5 and 1.5. For all lengths considered, the fit was reasonably good, with correlation coefficients always larger than 0.95. The obtained slopes are plotted against $1/N$ in Fig. 4. Although the errors are rather large, the data is compatible with the functional form $-\partial\beta/\partial\hat{c} = A_0^0 + A_1^0/N$. The parameters that we obtained by fitting this relationship are also compatible, within error bars, with those obtained from SCN data: We find, for PDB structures, $A_0^0 = 2.33 \pm 0.17$ and $A_1^0 = 117 \pm 25$. While a more careful study is still necessary on this issue, the present results seem to confirm this length effect on the amino acid distributions.

D. Conservation and designability

The results that we present imply that there is a direct relationship between a structural indicator, the principal eigenvector of the contact matrix, and site-specific measures of long-term evolutionary conservation and hence of limits in divergent evolutionary changes. This relationship also provides a link between the topology of a fold and its designability.

One convenient measure of the amino acid conservation at a given position is given by the rigidity, defined as

$$R_i = \sum_{\text{fag}} [\pi_i(a)]^2 = \frac{\sum_{\text{fag}} \exp[-2\beta h(a)]}{\sum_{\text{fag}} \exp[-\beta h(a)]}^2; \quad (11)$$

$R_i = 1$ means that the same amino acid is present at position i in all sequences, i.e. the conservation is total and $\beta_i^{-1} = 0$. In general, the rigidity decreases with increasing temperature

β_i j^1 . One can use Eqs. (7,11) to compute the rigidity from the principal eigenvector. However, the dependence becomes clearer when fitting directly the rigidity as a function of the principal eigenvector component. We did this on the data generated through the SCN model, finding that the best fit is parabolic and the three parameters depend on the protein length. Instead of the PE component c_i , we use the rescaled variable $x_i = \frac{c_i}{N c_i}$, which is normalized such that its mean squared value is one, i.e. $x^2 = N^{-1} \sum_i x_i^2 = 1$. Using this scaled variable, the rigidities of all proteins in our data set can be fitted by the expression

$$R_i^{\text{pred}} = A + \frac{B}{N^d} x_i - C x_i - \frac{D}{N} x_i^2; \quad (12)$$

with $A = 0.0630 \pm 0.0017$, $B = 0.28 \pm 0.16$, $C = 1.879 \pm 0.102$, $D = 5.36 \pm 0.89$, and $d = 0.47 \pm 0.11$. The factor $N^{-d} = N^{1/2}$ can be interpreted as a further indication that rigidities tend to become more homogeneous for larger proteins, as previously noted concerning the Boltzmann parameters. Eq. (12) predicts the rigidity for all the proteins that we studied with the SCN model, with an average root mean square relative error of around 10% and an average correlation coefficient between predicted and observed rigidities of 0.88 (cf. Table I). These values change very little in leave-one-out tests, where we discard one protein for estimating the parameters and then use it as a blind test.

A standard information-theoretic measure of site-specific sequence conservation is given by the entropy of the amino acid distribution,

$$S_i = \sum_{\text{fag}} \pi_i(a) \log [\pi_i(a)] = \log Z(\beta_i)] + \beta_i h_i \text{evol}; \quad (13)$$

where $Z(\beta_i) = \sum_a \exp(-\beta_i h_i(a))$. The entropy attains its maximum value, $S_i = \log(20)$, at $\beta_i = 0$ and it decreases with increasing β_i .

An important property of the entropy is that its exponential, $\exp(S_i)$, provides an estimate of the average number of amino acid types acceptable at position i over very long evolutionary times. The exponential of the sum of all site-specific entropies, $\exp(\sum_i S_i)$, gives an estimate of the sequence space compatible with a given fold, termed the designability of the fold, where we are assuming that the amino acid distributions at different positions are independent. Although this assumption is clearly oversimplified, the estimate of designability that can be obtained should be a valuable approximation, and our approach allows to connect it explicitly to a topological feature of the protein native structure (Koehl and Levitt, 2002; England and Shakhnovich, 2003).

IV. DISCUSSION AND CONCLUSIONS

We have predicted analytically that amino acids at specific positions are distributed according to a Boltzmann law. In the latter, the role of energy is played by the hydrophobicity, measured through an *interactivity* scale, and that of temperature by a quantity strongly correlated with a structural indicator, namely the corresponding component of the principal eigenvector of the native contact matrix (PE). This prediction, which does not involve any free parameter, is in very good

agreement both with simulations of the SCN model of protein evolution and with site-specific amino acid distributions that we obtained from a representative subset of single-domain globular proteins in the PDB.

The relationship between a structural profile (the PE) and an evolutionary profile (the Boltzmann parameters) that we find has an interesting interpretation. Positions with a large principal eigenvector component are strongly interacting with other positions in the core of the protein. Therefore, they preferentially host strongly hydrophobic amino acids (large negative β_i). On the other hand, positions with small PE are contained in loops and, with higher probability, they host polar amino acids (large positive β_i).

Despite this general interpretation, we have verified, using the SCN model of protein evolution, that the PE has the strongest predictive power among several similar structural indicators that quantify the difference between core and surface positions of a protein. As alternative structural indicators, we considered the total number of contacts, the number of long-range contacts (separated by more than 10 residues along the sequence) and the contact order (the average loop length of each contact involving a given site), and we correlated them with measures of site-specific conservation, but we always found a correlation significantly weaker than for the PE.

The distributions derived here refer to very long evolutionary times, when memory of the starting sequence has been lost. We recall the assumptions that we made for deriving the site-specific distributions. The first assumption is that selection on folding stability can be represented effectively as a maximal correlation between the hydrophobicity profile (HP) of sequences compatible with a given fold and the optimal HP of that fold, the latter basically coinciding with the PE. This assumption follows directly from an approximation of our effective free energy function with its principal (hydrophobic) component. The second assumption is that the average of the HP of selected sequences over very long evolutionary times has a correlation coefficient of unity with the PE, i.e. all other energetic contributions average out. The third assumption is that this correlation is the only relevant property of the site-specific amino acid distributions, in other words, these distributions are the distributions of maximal entropy whose site-specific averages have correlation of one with the PE, thus fulfilling the stability requirement. From these three assumptions the Boltzmann form of the amino acid distributions is straightforward. In order to compute the site-specific Boltzmann parameters, however, we still have to know the positional mean and standard deviation of the site-specific HPs. These quantities are determined by the mutation process and by the selection parameters. They can be computed directly from the data, in such a way that the analytic prediction does not contain any free parameter.

The Boltzmann distribution that we predicted for the hydrophobicity at a given site is functionally similar to distributions observed for other properties of native protein structures, as for instance for amino acid contacts (Miyazawa and Jernigan, 1985), and it may point out to an alternative or complementary explanation for such distributions. In a study related to the present one, for instance, Boltzmann statistics for structural elements were predicted in stable folds of globular proteins (Finkelstein et al., 1995).

Kinjo and Nishikawa have very recently pointed out the ex-

istence of a strong relationship between hydrophobicity and the main eigenvector of substitution matrices derived from protein alignments with various values of the sequence identity of the aligned proteins (Kinjo and Nishikawa, 2004). They looked at the eigenvector corresponding to the largest eigenvalue (in absolute value) of the substitution matrices. For high sequence identities (above 35 percent), this eigenvector indicates the propensity of the amino acid to mutate over short evolutionary times (mutability). For low sequence identities (below 35 percent), corresponding to long evolutionary times, this eigenvector is very strongly correlated with hydrophobicity. This correlation is easily understood in light of the result presented here. In fact, Kinjo and Nishikawa used the Henikoff's method (Henikoff and Henikoff, 1992) for deriving substitution matrices from observed frequencies of aligned amino acids at positions with various PE values. Using our notations, these substitution matrices can be indicated as $M(a;b) = \log \pi_i(a)\pi_i(b) = \pi_i(a) - \pi_i(b)$, where the angular brackets denote positional average. In other words, these substitution matrices measure the tendency of two residue types a and b to co-occur at the same sites. The relationship between large time substitution matrices and hydrophobicity gives therefore independent support to our main result.

In dealing with protein families generated from natural evolution, our approach has two main difficulties: First, it can not take into account functional conservation; second, a large number of sequence pairs separated by very long evolutionary time is required. Because of these difficulties, the site-specific conservation predicted by our model agrees only qualitatively with site-specific conservation observed in aligned protein families (Bastolla et al., 2003a). For tackling these difficulties, we tested our analytic predictions on a large set of proteins in the Protein Data Bank. Positions belonging to different protein folds were counted together in the same structural class characterized by the value of the normalized PE.

The agreement between the analytic prediction and the observed distributions may be surprising in view of the fact that Eq. (9) takes into account neither the genetic code nor the codon usage. It is known that the observed frequencies of amino acids correlate strongly with their number of synonymous codons, and even more strongly with their cumulative codon frequencies expected in the simple hypothesis that the three bases constituting each codon are independently distributed (Sueoka, 1961). Moreover, the frequency of nucleotides at coding positions correlate strongly with the frequency of nucleotides at non-coding positions such as the synonymous 3rd codon positions (Bernardi and Bernardi, 1986), which are thought to reflect the mutational process. On the other hand, mutations are neither adequately represented in the SCN model, which is a model at the amino acid level where all amino acid mutations are equiprobable.

The most straightforward way to include the biases of the mutational process is to modify Eq. (5) with $\pi_i(a) \propto w(a) \exp[-\beta h(a)]$, where the weights $w(a)$ are either the number of synonymous codons or their cumulative frequency, estimated using average nucleotide compositions. We will ad-

dress this issue in future work.

We also observed a length effect in the dependence of the Boltzmann parameters β_i on the PE. For longer proteins this dependence becomes weaker, approximately following a law of the type $A_0 + A_1 N$. This result holds for SCN simulations and, although less significantly, for frequency distributions obtained from the PDB. Formally, the result directly follows from the fact that the evolutionary average of the hydrophobicity, $h_i \text{ evol}$, varies less and less across different positions i for longer proteins. This length dependence of the HP is consistent with the fact that the position average of $h_i \text{ evol}$ decreases with chain length, i.e. the length of a protein influences its composition (White, 1992; Bastolla and Demetrius, submitted), such that longer proteins tend to become less hydrophobic. (We note, however, that these results were obtained using the interactivity scale, and they can not be significantly generalized to other hydropathy scales.) These results can be understood considering that longer proteins are stabilized by a larger number of interactions per residue. Selection for protein stability is therefore expected to be weaker on individual interactions. In support of this prediction, the average interaction energy per contact in PDB structures was found to decrease with chain length (Bastolla and Demetrius, submitted).

The site-specific amino acid frequencies that we derived may find applications in the estimation of site-specific substitution matrices (Liò and Goldman, 1998; Thorne, 2000; Fornasari et al., 2002), and site-specific structural conservation. Our approach may provide analytic understanding of the limits imposed by structural and functional constraints to the divergent evolution of protein sequences and of the reliability of phylogenetic reconstructions from protein sequences for anciently diverged taxa (Meyer et al., 1986). A better understanding of structural conservation may also improve the prediction of functional conservation at sites that appear more conserved than expected on a structural basis alone (Casari et al., 1995; Ota et al., 2003). The dependence of amino acid distributions on the PE that we presented here is also a step towards determining the structural determinants of protein 'designability' (Li et al., 1998; Helling et al., 2001; England and Shakhnovich, 2003), namely the volume of sequence space compatible with a given fold.

Acknowledgments

MP gratefully acknowledges financial support by the guest program of the Max-Planck-Institut für Physik komplexer Systeme in Dresden, Germany, during the early stages of this project. UB is sponsored by the I3P program of the Spanish CSIC co-financed by the European Social Fund. We gratefully acknowledge discussions with Alfonso Valencia, Julian Echave, and Gustavo Parisi, and correspondence with Akira Kinjo.

BASTOLLA, U., FRAUENKRON, H., GERSTNER, E., GRASSBERGER, P., and W. NADLER. 1998. Testing a new Monte Carlo algorithm for protein folding. *Proteins* **32**:52-66.

BASTOLLA, U., VENDRUSCOLO, M., and H.E. ROMAN. 1999. Neutral evolution of model proteins: Diffusion in sequence space and overdispersion. *J. Theor. Biol.* **200**:49-64.

BASTOLLA, U., VENDRUSCOLO, M., and H.E. ROMAN. 2000a. Structurally constrained protein evolution: Results from a lattice simulation. *Eur. Phys. J. B* **15**:385-397.

BASTOLLA, U., VENDRUSCOLO, M., and E.W. KNAPP. 2000b. A statistical mechanical method to optimize energy parameters for protein folding. *Proc. Natl. Acad. Sci. USA* **97**:3977-3981.

BASTOLLA, U., KNAPP, E.W., and M. VENDRUSCOLO. 2001. How to guarantee optimal stability for most protein native structures in the Protein Data Bank. *Proteins* **44**:79-96.

BASTOLLA, U., PORTO, M., ROMAN, H.E., and M. VENDRUSCOLO. 2002. Lack of self-averaging in neutral evolution of proteins. *Phys. Rev. Lett.* **89**:208101/1-208101/4.

BASTOLLA, U., PORTO, M., ROMAN, H.E., and M. VENDRUSCOLO. 2003a. Connectivity of neutral networks, overdispersion and structural conservation in protein evolution. *J. Mol. Evol.* **56**:243-254.

BASTOLLA, U., PORTO, M., ROMAN, H.E., and M. VENDRUSCOLO. 2003b. Statistical properties of neutral evolution. *J. Mol. Evol.* **57**:S103-S119.

BASTOLLA, U., PORTO, M., ROMAN, H.E., and M. VENDRUSCOLO. 2004. The principal eigenvector of contact matrices and hydrophobicity profiles in proteins. *Proteins*, in print.

BATEMAN, A., BIRNEY, E., DURBIN, R., EDDY, S.R., HOWE, K.L. and E.L.L. SONNHAMMER. 2000. The PFAM contribution to the annual NAR database issue. *Nucl. Ac. Res.* **28**:263-266.

BERNARDI, G. and G. BERNARDI. 1986. Compositional constraints and genome evolution. *J. Mol. Evol.* **24**, 1-11.

BRINGELSON J.D. and P.G. WOLYNES. 1987. Spin-glasses and the statistical-mechanics of protein folding. *Proc. Natl. Acad. Sci. USA* **84**:7524-7528.

CASARI G. and M.J. SIPPL. 1992. Structure-derived hydrophobic potential. Hydrophobic potential derived from X-ray structures of globular proteins is able to identify native folds. *J. Mol. Biol.* **224**:725-732.

CASARI, G., SANDER, C., and A. VALENCIA. 1995. A method to predict functional residues in proteins. *Nat. Struct. Biol.* **2**:171-178.

ENGLAND, J.L. and E.I. SHAKHNOVICH. 2003. Structural Determinant of Protein Designability. *Phys. Rev. Lett.* **90**:218101/1-218101/4.

FELSENSTEIN, J. 1981. Evolutionary trees from DNA sequences: A maximum likelihood approach. *J. Mol. Evol.* **17**:368-376.

FORNASARI, M.S., PARISI, G., and J. ECHAVE. 2002. Site-specific amino acid replacement matrices from structurally constrained protein evolution simulations. *Mol. Biol. Evol.* **19**:352-356.

GOLDSTEIN, R.A., LUTHEY-SCHULTEN Z.A., and P.G. WOLYNES. 1992. Optimal protein-folding codes from spin-glass theory. *Proc. Natl. Acad. Sci. USA* **89**:4918-4922.

GUTIN, A.M., ABKEVICH, V.I., and E.I. SHAKHNOVICH. 1995. Evolution-like selection of fast-folding model proteins. *Proc. Natl. Acad. Sci. USA* **92**:1282-1286.

HALPERN, A.L., and W.J. BRUNO. 1998. Evolutionary distances for protein-coding sequences: modeling site-specific residue frequencies. *Mol. Biol. Evol.* **15**:910-917.

HELLING, R., LI, H., MELIN, R., MILLER, J., WINGREEN, N., ZENG, C. and C. TANG. 2001. The designability of protein structures. *J. Molecular Graphics & Modelling* **19**:157-167.

HENIKOFF, S., and J.G. HENIKOFF. 1992. Amino acid substitution matrices from protein blocks. *Proc. Natl. Acad. Sci. USA* **89**:10915-10919.

HENIKOFF, S., and J.G. HENIKOFF. 1993. Performance evaluation of amino acid substitution matrices. *Proteins* **17**:49-61.

HOBOHM, U. and C. SANDER. 1994. Enlarged representative set of protein structure. *Protein Sci* **3**:522-524.

HOLM, L. and C. SANDER. 1996. Mapping the protein universe. *Science* **273**:595-602.

JONES, D.T., TAYLOR, W.R. and J.M. THORNTON. 1992. The rapid generation of mutation data matrices from protein sequences. *Comp. Appl. Biosci.* **8**:275-282.

KINJO, A.R. and K. NISHIKAWA. 2004. Eigenvalue analysis of amino acid substitution matrices reveal a sharp transition of the mode of sequence conservation in proteins. *Bioinformatics*, DOI:10.1093/bioinformatics/bth297.

KLIMOV, D.K. and D. THIRUMALAI. 1996. Factors governing the foldability of proteins. *Proteins* **26**:411-441.

KOEHL, P. and M. LEVITT. 2002 Protein topology and stability define the space of allowed sequences *Proc. Natl. Acad. Sci. USA* **99**:1280-1285.

LI, H., TANG, C., and N.S. WINGREEN. 1997. Nature of driving force for protein folding: A result from analyzing the statistical potential. *Phys. Rev. Lett.* **79**:765-768.

LI, H., TANG, C., and N.S. WINGREEN. 1998. Are protein folds atypical? *Proc. Natl. Acad. Sci. USA* **95**:4987-4990.

LIÒ, P. and N. GOLDMAN. 1998. Models of molecular evolution and phylogeny. *Genome Res.* **8**:1233-1244.

MEYER, T.E., CUSANOVICH, M.A., and KAMEN, M.D. 1986. Evidence against use of bacterial amino acid sequence data for construction of all-inclusive phylogenetic trees *Proc. Natl. Acad. Sci. USA* **83**:217-220.

MIYAZAWA, S. and R.L. JERNIGAN. 1985. Estimation of effective inter-residue contact energies from protein crystal structures: Quasi-chemical approximation. *Macromolecules* **18**:534-552.

OTA, M., KINOSHITA, K., and K. NISHIKAWA. 2003. Prediction of catalytic residues in enzymes based on known tertiary structure, stability profile, and sequence conservation. *J. Mol. Biol.* **327**:1053-1064.

OVERINGTON, J., JOHNSON, M.S., SALI, A., and T.L. BLUNDELL. 1990. Tertiary structural constraints on protein evolutionary diversity - templates, key residues and structure prediction. *Proc. Roy. Soc. Lond. B* **241**:132-145.

PARISI, G. and J. ECHAVE. 2001. Structural constraints and emergence of sequence patterns in protein evolution. *Mol. Biol. Evol.* **18**:750-756.

PORTO, M., BASTOLLA, U., ROMAN, H.E., and M. VENDRUSCOLO. 2004. Reconstruction of protein structures from a vectorial representation. *Phys. Rev. Lett.* **92**:218101/1-218101/4.

PTITSYN, O.B. 1998. Protein folding and protein evolution: Common folding nucleus in different subfamilies of c-type cytochrome? *J. Mol. Biol.* **278**:655-666.

PTITSYN, O.B. and K.H. TING. 1999. Non-functional conserved residues in globins and their possible role as a folding nucleus. *J. Mol. Biol.* **291**:671-682.

SUEOKA, N. 1961. Correlation between base composition of the deoxyribonucleic acid and amino acid composition of proteins. *Proc. Natl. Acad. Sci. USA* **47**, 469-478.

THORNE, J.L. 2000. Models of protein sequence evolution and their applications. *Curr. Opin. Genet. Dev.* **10**:602-605.

WHITE, S.H. 1992. Amino acid preferences of small proteins. Implications for protein stability and evolution. *J. Mol. Biol.* **227**:991-995.